

Bose-Einstein Condensation of $S = 1$ Ni spin degrees of freedom in $\text{NiCl}_2\text{-4SC}(\text{NH}_2)_2$

V. S. Zapf,¹ D. Zocco,¹ M. Jaime,¹ N. Harrison,¹ A. Lacerda,¹ C. D. Batista,² A. Paduan-Filho,³

¹*National High Magnetic Field Laboratory, Los Alamos, NM*

²*Condensed Matter and Statistical Physics, Los Alamos National Laboratory, Los Alamos, NM*

³*Instituto de Fisica, Universidade de Sao Paulo, Sao Paulo, Brazil*

(Dated: November 5, 2018)

It has recently been suggested that the organic compound $\text{NiCl}_2\text{-4SC}(\text{NH}_2)_2$ (DTN) exhibits Bose-Einstein Condensation (BEC) of the Ni spin degrees of freedom for fields applied along the tetragonal c -axis. The Ni spins exhibit 3D XY-type antiferromagnetic order above a field-induced quantum critical point at $H_{c1} \sim 2$ T. The Ni spin fluid can be characterized as a system of effective bosons with a hard-core repulsive interaction in which the antiferromagnetic state corresponds to a Bose-Einstein condensate (BEC) of the phase coherent $S = 1$ Ni spin system. We have investigated the the high-field phase diagram and the occurrence of BEC in DTN by means of specific heat and magnetocaloric effect measurements to dilution refrigerator temperatures. Our results indicate that a key prediction of BEC is satisfied; the magnetic field-temperature quantum phase transition line $H_c(T) - H_{c1} \propto T^\alpha$ approaches a power-law at low temperatures, with an exponent $\alpha = 1.47 \pm 0.06$ at the quantum critical point, consistent with the BEC theory prediction of $\alpha = 1.5$.

PACS numbers: 75.40.-s,65.40.Ba,

Keywords: Bose-Einstein condensation, Ni systems, quantum critical point

In the past few years, a class of quantum spin systems that exhibit a Bose-Einstein condensation in applied magnetic fields has been receiving an increasing amount of attention. The compounds studied previously consist of chains of Ni atoms,^{1,2,3} planes of Cu dimers, (BaCuSiO_6)^{4,5} or 3-D coupled spin ladders (TlCuCl_3 and KCuCl_3).^{6,7} In these compounds, the spin degrees of freedom are generally provided by either weakly interacting $S = 1$ Ni chains exhibiting a Haldane gap, or by a lattice of dimerized $S = 1/2$ Cu^{2+} ions. The spin singlet ground state of these systems is separated from the lowest excited state (triplet) by a finite energy gap at zero magnetic field. In the presence of a magnetic field, the Zeeman term reduces the energy of the $S = -1$ triplet state, until it reaches the energy of the non-magnetic ground state at a field H_{c1} . Canted XY antiferromagnetism is then observed between H_{c1} and an upper critical field H_{c2} . This XY antiferromagnetic phase of $S = 1$ spins has a $U(1)$ symmetry and can thus be interpreted as a BEC. The $U(1)$ symmetry requires a spin environment that is axially symmetric with respect to the applied field. Observation of a gapless Goldstone mode (magnons) in the ordered phase could in principle provide evidence of a broken continuous $U(1)$ symmetry. Inelastic neutron scattering measurements of the compound TlCuCl_3 were proposed to be consistent with this interpretation.⁶ However, ESR measurements subsequently revealed significant magnetic anisotropy in this compound inconsistent with a $U(1)$ symmetry of the spins.⁸ In general, axial symmetry is not expected for weakly coupled spin ladder and spin chain systems.

The compound $\text{NiCl}_2\text{-4SC}(\text{NH}_2)_2$ (DTN)⁹ is a new candidate for Bose-Einstein condensation of spins, and has several features that make it unique among these BEC of spin systems. In a similar manner to $\text{BaCuSi}_2\text{O}_6$, the tetragonal crystal symmetry satisfies the $U(1)$ symmetry requirement for BEC with the additional feature

that the symmetry can be tuned by rotating the applied magnetic field. It has been predicted¹⁰ that an XY magnet should occur for fields along the c -axis, and an Ising magnet for angles up to 40 degrees away from the c -axis. The spin configuration is also different from previous BEC compounds, consisting only of a spin-one state with no spin-singlet state. The tetragonal spin lattice provided by the Ni ions is described by the Hamiltonian:

$$\mathcal{H} = \sum_{\mathbf{j}, \nu} J_\nu \mathbf{S}_{\mathbf{j}} \cdot \mathbf{S}_{\mathbf{j}+\mathbf{e}_\nu} + D \sum_{\mathbf{j}} (S_{\mathbf{j}}^z)^2, \quad (1)$$

where $\nu = \{a, b, c\}$ and $J_a = J_b$ due to the tetragonal symmetry of the crystal structure. The single ion anisotropy $D \sim 10$ K^{10,11} splits the the Ni $S = 1$ spin state into the $S_z = 0$ ground state and the $S_z = \pm 1$ excited states. Thus, for an applied magnetic field along the c -axis, the level crossing occurs between two triplet states rather than a triplet and a singlet as is the case for all other BEC systems studied to date. Magnetization measurements⁹ have revealed AFM order between $H_{c1} \sim 2$ T and $H_{c2} \sim 12$ T with a maximum Néel temperature of 1.2 K. For a magnetic field perpendicular to the c axis, no transition is observed up to $H = 15$ T since such a field mixes the $S_z = 0$ state with a linear combination of the $S_z = \pm 1$ states, producing an effective repulsion between energy levels that precludes any field-induced quantum phase transition.

In this work, we investigate the temperature-magnetic field phase diagram for $H \parallel c$ via thermodynamic measurements. A key prediction of the BEC theory is a power-law temperature dependence of the phase transition line $H_c(T) - H_{c1} \propto T^\alpha$ where $\alpha = 1.5$.¹² Previous studies on DTN and other candidate BEC spin systems have found a wide variety of values of α , generally higher than the predicted value of 1.5. This is due to the fact that the fits are performed at relatively high temperatures, whereas the power-law universal behavior is only

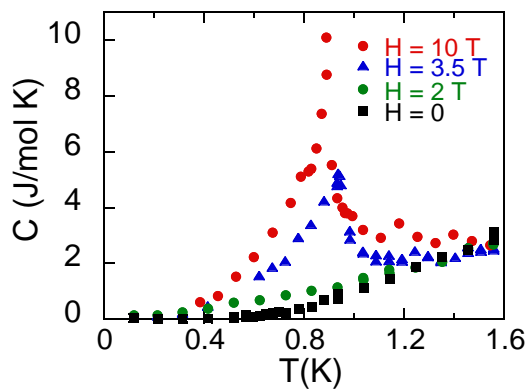


FIG. 1: Specific heat C versus temperature T of $\text{NiCl}_2\text{-4SC}(\text{NH}_2)_2$ for $H \parallel c$ in applied magnetic fields of 0, 2, 3.5, and 10 T.

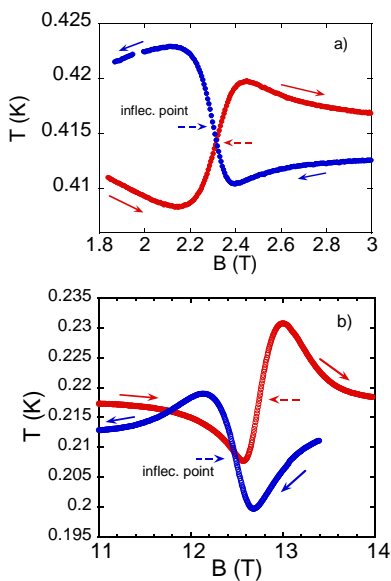


FIG. 2: Magnetocaloric effect data determined by monitoring T while sweeping B up and down. Solid arrows indicate the direction of B and dashed arrows indicate the inflection point in T versus B .

valid for $T_c \rightarrow 0$.⁵ Furthermore, the value of α is very dependent on the value of H_{c1} chosen for the fit, which is difficult to extrapolate from higher temperature data. A previous work found $\alpha = 2.6$ from fits to magnetization data on DTN with most of the data lying between 0.5 and 1.5 K.⁹ In this present study, we obtain α from specific heat and magnetocaloric effect measurements to dilution refrigerator temperatures. We determine the value of α using the extrapolation method described by Sebastian *et al.*⁵ The validity of this extrapolation has been verified using Monte Carlo calculations of $H_c(T)$ and the method has been successfully used to obtain the exponent for the compound $\text{BaCuSi}_2\text{O}_6$.⁵

Specific heat and the magnetocaloric effect (MCE) were measured in a dilution refrigerator system with

an 18 T magnet at the National High Magnetic Field Laboratory in Los Alamos, NM. All measurements were conducted on single crystals with the external field oriented along the tetragonal c -axis. Specific heat ($100 \text{ mK} \leq T \leq 1.5 \text{ K}$) was determined by the quasi-adiabatic heat pulse relaxation method, and the magnetocaloric effect was measured by sweeping the field up and down at 0.1 T/min while monitoring the temperature between 80 mK and 1.5 K .

Distinct thermodynamic transitions can be observed in the specific heat and magnetocaloric effect data at magnetic fields between 2.1 and 12.7 T. Representative data is shown in Figs 1 and 2 and the phase diagram determined from these data is shown in Fig. 3. The specific heat data shown in Fig. 1 exhibits sharp peaks for $H = 3.5 \text{ T}$ and 10 T . These peaks resemble the λ -like transition of the specific heat in superfluid helium, an archetypal BEC system. Detailed theoretical predictions for this system are necessary to make a precise comparison. An equal entropy construction was used to determine the midpoint of the transition. For transitions occurring at a given temperature, the specific heat transition at high fields shows a taller peak in the specific heat than the transition at low fields.

In the magnetocaloric effect data shown in Fig. 2, heating is observed as the magnetic field is swept through the AFM transition, surrounded by regions of cooling before and after the transition. The region of cooling after the transition can be attributed to a relaxation towards the bath temperature of the system. However, the cooling preceding the transition must be due to the sample. The inflection point of the $T(B)$ curve, corresponding to the point of maximum heat, was identified as the phase transition. The data at high field shown in Fig. 2(b) shows hysteresis between the up and down sweep of the field. This hysteresis is observed in the high field branch of the phase diagram for temperatures less than 0.6 K , and is discussed in greater detail later. The transition temperatures determined from specific heat and MCE are in excellent agreement as shown in Fig. 3. A second order phase transition such as the AFM transition we are expecting in this compound, should exhibit heating when entering the ordered phase, and cooling when leaving it. However, all of the MCE data shows heating in both directions when the field is swept up and down. This may indicate a coupling to the lattice that results in an apparent first-order phase transition.

The resulting phase diagram (Fig. 3) shows an ordered phase occurring between $H_{c1} \sim 2.1 \text{ T}$ and $H_{c2} \sim 12.7 \text{ T}$ with a maximum critical temperature of $T_c = 1.2 \text{ K}$. The values of H_{c1} and H_{c2} extracted from this phase diagram are in agreement with those determined from magnetization to within a few percent.⁹ The discrepancy could be due to slight orientation errors of the sample and the fact that in the work by Paduan-Filho *et al.*, the onset of the transition is determined from the peak in the first derivative of $M(H)$, whereas a comparison with the midpoint of the transition in the specific heat and

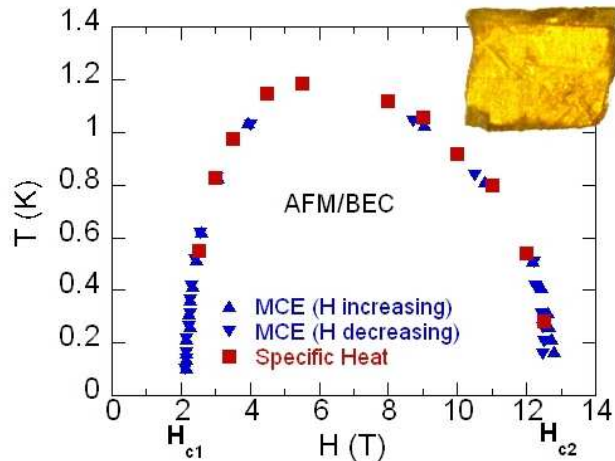


FIG. 3: Temperature T - Magnetic field H phase diagram from specific heat and magnetocaloric effect data. Bose-Einstein Condensation (BEC)/canted antiferromagnetic order (AFM) is thought to occur in the area under the symbols. Top right: Photograph of the single crystal of DTN used in this work. The plane of the paper is the $a - b$ plane of the crystal.

MCE effect would require taking the inflection point, or the peak in the second derivative of $M(H)$.

The values of H_{c1} and H_{c2} for $H \parallel c$ can be obtained as a function of D and J_ν using a generalized spin-wave approach^{10,13}:

$$g\mu_B H_{c1} = \sqrt{D^2 - 2zDJ} \quad (2)$$

$$g\mu_B H_{c2} = D + 2zJ, \quad (3)$$

where the coordination number $z = 6$. Here J is the average of J_ν over the three different directions $J = \frac{1}{3}(2J_a + J_c)$. The gyromagnetic ratio g_c has been determined from fits to the magnetization versus temperature as $g_c = 2.26$ for $H \parallel c$. Thus D and J can be solved for yielding $D/k_B = 10.23$ K and $J/k_B = 0.77$ K. In contrast to $\text{BaCuSi}_2\text{O}_6$, the DTN compound is in a regime for which a two level description does not work because $2zJ/D \sim 1$. In other words, the fluctuations to the high energy $S_z = -1$ state play a role even at very low energies. Consequently, the phase diagram is not symmetric around the maximum critical field H_{max} (see Fig. 3). The asymmetry is also manifested as a difference between the size of the specific heat jumps at low and high fields for a given critical temperature, as shown in Fig. 1.

In addition to the asymmetry in the shape of the $H_c(T)$ curve, the MCE data shows hysteresis for $T < 0.6$ K in the high field branch of the phase diagram. Furthermore, an anomalous feature can be observed in magnetization $M(H)$ data taken by Paduan-Filho *et al*⁹ at $T = 16$ mK and to a lesser degree at $T = 0.6$ K. Between $H_{c1} \sim 2$ T and $H \sim 10$ T, the $M(H)$ data is linear as expected for a BEC. However, above $H = 10$ T, the slope of M versus

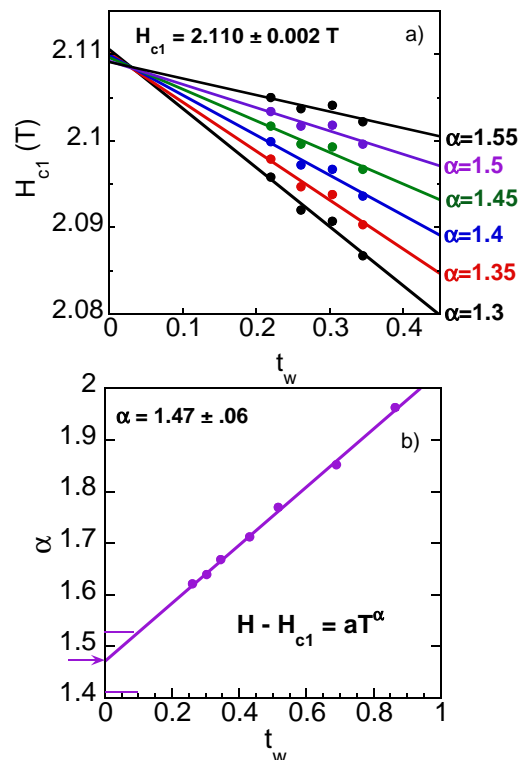


FIG. 4: Estimation of the power-law exponent α by fits over varying temperature ranges $t_w = \Delta T/1.2$ K (see text). a) Fits of the expression $H_c(T) - H_{c1} \propto T^\alpha$ were performed for various fixed values of α at various temperature ranges, resulting in H_{c1} a function of temperature range t_w . The extrapolated value of H_{c1} at zero temperature is $H_{c1} = 2.110 \pm .002$ T. b) Using the value of H_{c1} determined in the left figure, fits to $H_c(T) - H_{c1} \propto T^\alpha$ are performed for various temperature range to determine α , and α is shown versus t_w . The extrapolated value of α at $t_w = 0$ is indicated by the arrow, and the lines indicate the error bar.

H increases until M saturates above H_{c2} . Thus, there is a region of anomalous behavior from thermodynamic and magnetization measurements between $H = 10$ T and H_{c2} , and below $T = 0.6$ K. One possible explanation is a gradual expansion in the lattice beginning near $H = 10$ T. At high magnetic fields approaching H_{c2} , the uniform magnetization along the c -axis becomes large in competition with the antiferromagnetic exchange interaction J . Thus, the system can lower its energy by increasing the Ni-Ni distance to lower J . As a result, $M(H)$ would saturate more rapidly with applied magnetic field. The transition from the AFM phase back to the paramagnetic phase at high fields would be accompanied by an abrupt cessation of the lattice strain, consistent with the hysteretic first-order transition observed in the MCE effect at high fields. Further studies, such as magnetostriction are necessary to investigate this possibility.

In order to study the occurrence of BEC of the Ni spins in DTN, we examine the temperature dependence of the AFM phase transition line near H_{c1} . As men-

tioned previously, a power-law temperature dependence $H_c(T) - H_{c1} \propto T^\alpha$ where $\alpha = 1.5$ is predicted for a transition to a BEC phase. In our fits to the $H_c(T)$ data for the compound DTN, we limit ourselves to investigating the low field side of the phase diagram due to the possibility of a magnetically induced strain phase occurring at high fields. The value of α is closely dependent on the value of H_{c1} , as well as on the temperature range of the fit. α is expected to approach 1.5 only as $T \rightarrow 0$. The lack of particle-hole symmetry does not allow us to use the relation $t \sim (1 - h^2)^\nu g(h^2)$ ($\nu = 1/\alpha$, $t = T_c/T_{max}$ and $h = \frac{H_{max} - H}{H_{max} - H_{c1}}$) that was exploited to determine the exponent α for BaCuSi₂O₆.⁵ Therefore, we use the simplest power law expression: $H_c(T) - H_{c1} \propto T^\alpha$.

As a first step, we fix α and fit the $H_c(T)$ data to determine H_{c1} . This fit is performed for data up to a maximum temperature where the window size $t_w = T_{max}/1.2K$. The fits are then repeated for different trial values of α . The results of these fits are shown in Fig. 4 (left). For each value of α , the H_{c1} values as a function of the window size t_w can be fit to a straight line and extrapolated to a window size $t_w = 0$. The extrapolations of $H_{c1}(t_w)$ for the different values of α converge near $t_w = 0$, resulting in a mean value of $H_{c1} = 2.110 \pm 0.002$ T.

In the expression $H_c(T) - H_{c1} \propto T^\alpha$, H_{c1} can now be fixed at 2.11 T and the $H_c(T)$ data is fit to determine α as a function of window size as shown in Fig. 4 (right). For

$t_w = 0$, α extrapolates to $\alpha = 1.47 \pm 0.06$ where the error bar in α results from the error bar in H_{c1} . This value is within experimental error of the predicted exponent $\alpha = 1.5$ for a Bose-Einstein condensate. Thus our data is consistent with a Bose-Einstein condensation of the Ni spin degrees of freedom.

In summary, we have mapped the high-field phase diagram of DTN using specific heat and magnetocaloric effect data, yielding a magnetic ordered state between $H_{c1} = 2.1$ T and $H_{c2} = 12.7$ T with a maximum critical temperature of 1.2 K. An anomalous region of the phase diagram is observed between $H \sim 10$ and 12.7 T and below $T \sim 0.6$ K possibly associated with lattice strain. The phase transition line near the quantum critical point at H_{c1} can be fit by the expression $H_c(T) - H_{c1} \propto T^\alpha$, resulting in a value of $\alpha = 1.47 \pm 0.06$, which is consistent with the predicted exponent equal to 1.5 for a quantum phase transition to a BEC.

Acknowledgments

This work was supported by the DOE and the NSF through the National High Magnetic Field Laboratory and the LANL Director-Funded Postdoctoral program. A.P.F. acknowledges support from CNPq (Conselho Nacional de Desenvolvimento Científico e Tecnológico, Brazil).

¹ Z. Honda, K. Katsumata, H. A. Katori, K. Yamada, T. Ohishi, T. Manabe, and M. Yamashita, *J. Phys.: Condens. Matter* **9**, L83 (1997).
² N. Tateiwa, M. Hagiwara, H. Aruga-Katori, and T. C. Kobayashi, *Physica B* **329-333**, 1209 (2003).
³ H. Tsujii, Z. Honda, B. Andraka, K. Katsumata, and Y. Takano, cond-mat/0409190].
⁴ M. Jaime, V. F. Correa, N. Harrison, C. D. Batista, N. Kawashima, Y. Kazuma, G. A. Jorge, R. Stern, I. Heinmaa, S. A. Zvyagin, et al., *Phys. Rev. Lett* **93**, 087203 (2004).
⁵ S. E. Sebastian, P. A. Sharma, M. Jaime, N. Harrison, V. Correa, L. Balicas, N. Kawashima, C. D. Batista, and I. R. Fisher, submitted to *Phys. Rev. Lett*; [cond-mat/0408100].
⁶ C. Rüegg, N. Cavadini, A. Furrer, H.-U. Güdel, K. Krämer, H. Mutka, A. Wildes, K. Habicht, and P. Vorderwisch, *Nature* **423**, 62 (2003).
⁷ A. Oosawa, T. Takamasu, K. Tatani, H. Abe, N. Tsujii, O. Suzuki, H. Tanaka, G. Kido, and K. Kindo, *Phys. Rev. B* **66**, 104405 (2002).
⁸ V. N. Glazkov, A. I. Smirnov, H. Tanaka, and A. Oosawa, *Phys. Rev. B* **69**, 184410 (2004).
⁹ A. Paduan-Filho, X. Gratens, and N. F. Oliveira, *Phys. Rev. B* **69**, 020405R (2004).
¹⁰ C. D. Batista, to be published.
¹¹ A. Paduan-Filho, R. D. Chirico, K. O. Joung, and R. L. Carlin, *J. Chem. Phys.* **74**, 4103 (1981).
¹² I. Affleck, *Phys. Rev. B* **43**, 3215 (1991).

¹³ H.-T. Wang and Y. Wang, *Phys. Rev. B* **71**, 104429 (2005).